NUMERICAL AND EXPERIMENTAL ANALYSIS OF HIGH-VELOCITY IMPACT BEHAVIOUR OF CARBON FIBRE REINFORCED THERMOPLASTIC COMPOSITES

M. A. A. Mohsin[1], L. Iannucci[1] and E. Greenhalgh[1]

[1]Imperial College London, Department of Aeronautics, Imperial College London, Exhibition Road, London SW7 2AZ, United Kingdom
[1]Email: m.mohsin14@imperial.ac.uk, Web Page: http://www.imperial.ac.uk

Keywords: high-velocity impact, high-performance composites, composite structures

Abstract

The low, medium and high-velocity impact resistance of fibre reinforced thermoplastic and thermosetting composites have continually attracted interest in automotive, aerospace and military applications. This research aims to characterise the high-velocity impact (HVI) response of a carbon fibre reinforced thermoplastic (CFRTP) composite system which is comprised of non-crimp fabric (NCF) biaxial 0/90 T700 carbon pre-impregnated with polyphenylene sulphide (PPS) thermoplastic (TP) veils. The raw materials were provided by THERMOCOMP [1] and the composite panels were manufactured using a 40-tonne hydraulic laboratory press via thermoforming process. The HVI tests were performed with velocities ranging from 130 to $250 m/s$. The projectile used is a $16 mm$ diameter spherical stainless steel with a mass of $16.5 \pm 0.5 g$. The entry and exit velocities were measured to determine the V_{50} and the energy absorbed in cases where perforation occurs. The experimental procedure was then numerically simulated using a finite element (FE) solver LS-DYNA®. The numerical model is then validated and compared against the experimental gatherings with respect to the exit velocities and damage mechanism.

1. Introduction

1.1. Background

Modern developments in the automotive and aerospace industry target optimised and improved composite performance. In addition to conventional quasi-static loading conditions typically associated with composite materials such as tension, compression and shear, some structural components have specific requirements in relation to impact damage resistance caused by foreign objects. This includes the impact damage caused by a ricochet of loose gravels on a car on the motorway or aircraft structures exposed to bird strike or runway debris. Hence, it is crucial to characterise the HVI response to determine the suitable composite material for such structural components. This would minimise the extent of damage of such structures and ensure safe operation. The physical phenomena observed in HVI on composite laminates are complex as it includes bending, fibre fracture, matrix cracking, delamination, etc. The HVI research of composites have largely focussed of thermosets (TS) instead of TP composites.

1.2. Non-crimp Fabric (NCF) Biaxial T700/PPS Composites

The idea of developing NCF reinforcement instead of conventional textiles began in 1982 [2]. It was designed as an alternative and more cost effective solution to conventional textiles [2]. The manufacturing process of NCF composites involve highly automated techniques which include stitching, weaving,

braiding and knitting [3]. Typical production techniques include bi-, tri- and quadriaxial fabrics of glass or carbon fibre using aramid warp knitting yarns.

The NCF biaxial 0/90 T700 carbon/PPS was supplied in the form of prepreg rolls. The panels were manufactured using hand lay-up technique and processed via thermoforming method using a 40-tonne hydraulic press (Fig. 1). In total, each plate consists of 24 plies of the prepregs i.e. $[(0/90)_{12}(90/0)_{12}]$. Once processed, the panels were cut into the required sample geometry and dimensions (Fig. 2) using a waterjet cutter. The density of the T700/PPS composite was measured using a pycnometer and its fibre-volume-fraction (FVF) was measured via thermogravimetric analysis (TGA). The physical and mechanical properties of the T700/PPS composite are described in Table 1.

Figure 1. 40-tonne Höfer hydraulic press at Imperial College London

Table 1. Physical and Mechanical Properties T700/PPS [4–6]

Properties	Value
Density, $\rho(kgm^{-3})$	1553
FVF, $V_f(\%)$	60.8
Tensile Strength (MPa)	852
Tensile Young's Modulus (GPa)	59.8
In-plane Shear Modulus (GPa)	3.3
Mode I Interlaminar Fracture Toughness, $G_{Ic}(kJm^{-2})$	1.75
Mode II Interlaminar Fracture Toughness, $G_{IIc}(kJm^{-2})$	1.41
Translaminar Fracture Toughness, $G_{Ic}^{T}(kJm^{-2})$	310

2. High-Velocity Impact (HVI) Test

To the authors' best knowledge, no information on the HVI response of the NCF T700 carbon/PPS is available in the open literature.

2.1. Experimental Method and Setup

The impact testing was conducted using a $16mm$ diameter spherical steel projectile (Fig. 3) at various velocities to achieve complete penetration of the target. This was achieved using the gas gun (Fig. 4) located in the structures lab at Imperial College London. The dimensions of the impact panel and impact location are shown in Fig. 2, where the sides of the $4mm$-thick rectangular panel measure $100mm \times 150mm$.

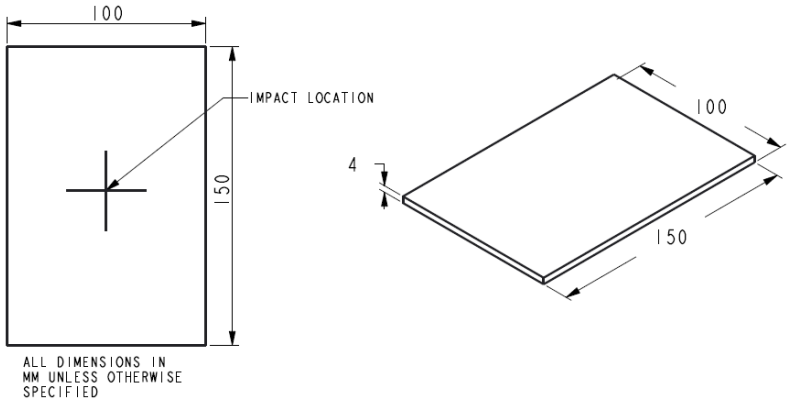

Figure 2. The dimensions of the HVI specimen

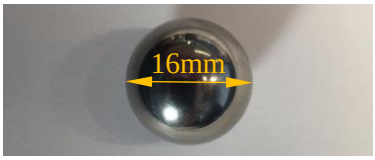

Figure 3. The 16mm diameter spherical AISI 52100 alloy stainless steel projectile

Figure 4. Imperial College gas gun; capture chamber (left) and breech (right) [7]

2.2. Data Reduction

The ballistic limit, V_{50} of the T700/PPS composite was estimated using the bisection method due to the limited number of specimens available and the fact that it is the most appropriated technique considering cost, accuracy and reliability. Upon determining the interval in which the V_{50} is to be found, based on the bisection method [8], the panels must be impacted at the average velocities at which complete and incomplete perforation occur. V_{50} represents the statistical velocity at which the probability of the projectile to thoroughly perforate the impact panel is 50%. With reference to the Jonas-Lambert model [9], the ballistic experimental data were fitted using Eq. 1

$$V_r = \begin{cases} 0, & 0 < V_i \leq V_{50} \\ \kappa \sqrt[p]{V_i^p - V_{50}^p}, & V_i > V_{50} \end{cases} \quad (1)$$

where V_i is the initial velocity of the projectile, V_{50} is the ballistic limit velocity, κ and p are the ballistic Jonas-Lambert parameters. The power, $p = 2$ for non-deformable rigid projectiles. Eq. 1 is known as the Recht-Ipson model [10]. Since the projectiles used in this study did not exhibit any deformation, the power, $p = 2$ and the parameter $\kappa = 1.192$ to fit the experimental results, which was obtained using the curve fitting tool on MATLAB®.

3. Numerical Model of the High-Velocity Impact (HVI) Test

The FE model of the HVI test consisted of a spherical impact and a composite plate with no boundary conditions as the forces exerted by the strings used to restrain the movement of test panel are negligible. The input parameters for the composite panel FE model (Fig. 5) are as listed in Table 1. The physical and mechanical properties such as the projectile's density, modulus, Poisson's ratio, etc. are shown in Table 2.

The FE model of the composite panel was constructed using four layers of continuum shell elements (TSHELL) with six integration points in each layer to represent the total of 24 plies of the NCF T700/PPS composite system. Three cohesive surfaces in between those four plies were used to simulate the TP veils in the composite plate. This was achieved using the AUTOMATIC_SURFACE_TO_SURFACE_TIEBREAK contact algorithm. The material card used to predict the composite's panel behaviour was the energy-based MAT_262-LAMINATED_FRACTURE_DAIMLER_CAMANHO. The elastic material card, MAT_001-ELASTIC was used to simulate the projectile and the interaction between the projectile and plate was modelled using the AUTOMATIC_SURFACE_TO_SURFACE_CONTACT algorithm in LS-DYNA®.

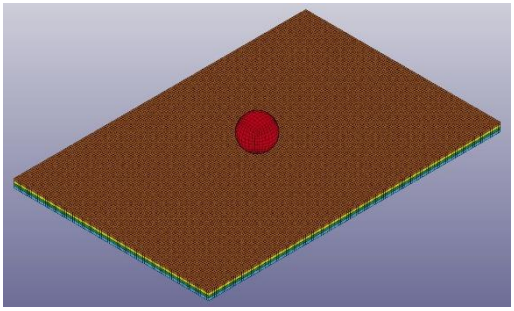

Figure 5. The FE model of the panel created in LS-DYNA®

Table 2. Physical and Mechanical Properties the AISI 52100 Alloy Stainless Steel Projectile

Properties	Value
Density, $\rho(kgm^{-3})$	7810
Poisson's ratio	0.27 - 0.30
Elastic Modulus (GPa)	190 - 210
Shear Modulus (GPa)	80
Bulk Modulus (GPa)	140

4. Results & Discussion

Fig. 6 illustrates the timelapse of the HVI test where penetration i.e. perforation did not occur. Experimentally, this was achieved at the initial velocity, $V_i = 156.3m/s$. The FE simulation on the other hand, indicated that the maximum initial velocity at which perforation did not occur was $V_i = 131.4m/s$. Hence, the experimental and numerical ballistic limits, V_{50} of the T700/PPS are $156.3m/s$ and $131.4m/s$, respectively (Fig. 6). Fig. 7 represents the timelapse of one of the HVI tests where perforation occurs, in this example, the initial velocity, $V_i = 211.1m/s$.

The ballistic curves and V_{50} for the T700/PPS obtained from the experiments and FE simulations are shown in Fig. 8a and comparison with a relatively good ballistic composite material, Vectran® is depicted in Fig. 8b. Fig. 9a illustrates the ballistic limit, V_{50} gathered from the experiments. Fig.9b represents the impact energy absorbed by the individual panels post impact, which was calculated from either the initial or the difference between initial and residual velocities from both, experiments and FE simulations.

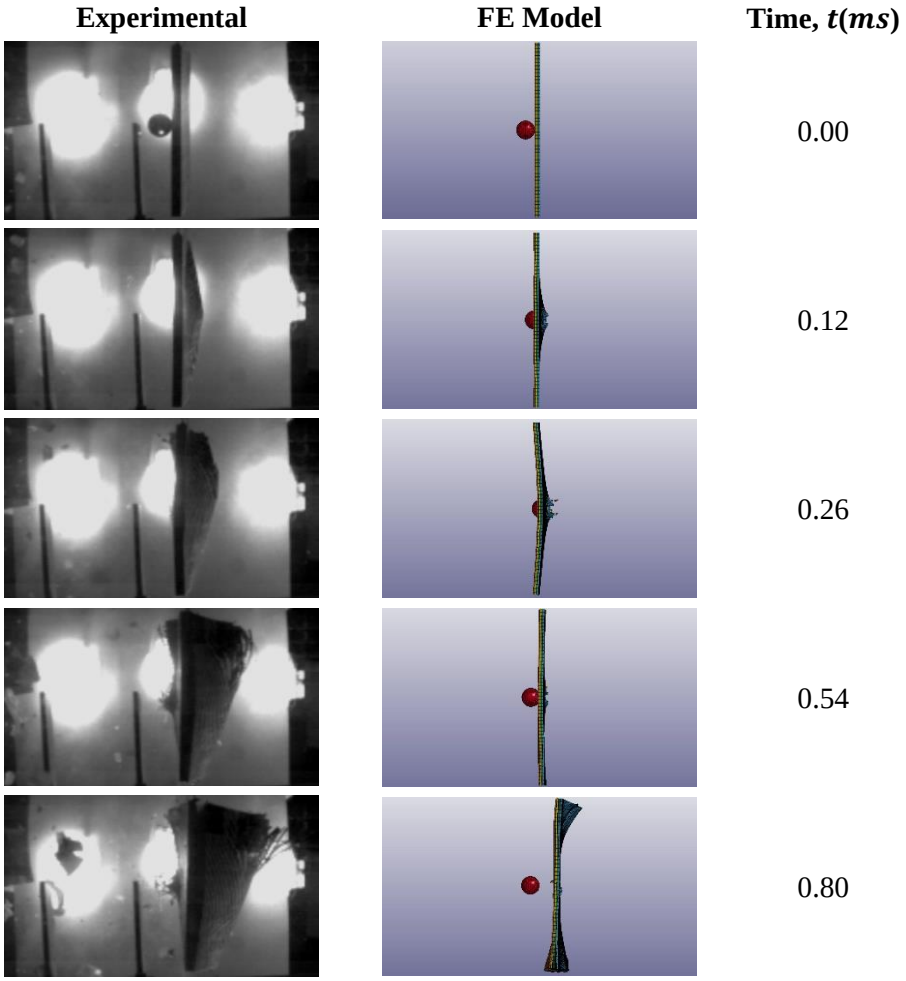

Figure 6. Timelapse of one of the HVI tests where perforation did not occur: $V_i = V_{50} = 156.3m/s$ in the experiment and $V_{50} = 131.4m/s$ in the FE simulation

The discrepancies within the experimental results based on the impact energy absorbed shown in Fig.9b (coefficient of variation, CV=22%), were caused predominantly by the quality of manufacturing process. The manufacturing process conducted in the laboratory is not ideal and far for being perfect. The prepregs (NCF carbon with TP veils) are very delicate and it was not easy to ensure that fibres are intact and in line by hand lay-up process, which in turn contributed a degree of defects in the manufactured panels. Hence, there is a scatter in the mechanical properties of the panel, contributing to the variations in the experimental results (Table 3). Since HVI is a complex phenomenon and in fact, governed by these characteristic properties, it is unsurprising that the CV of the experimental gatherings is about 22%.

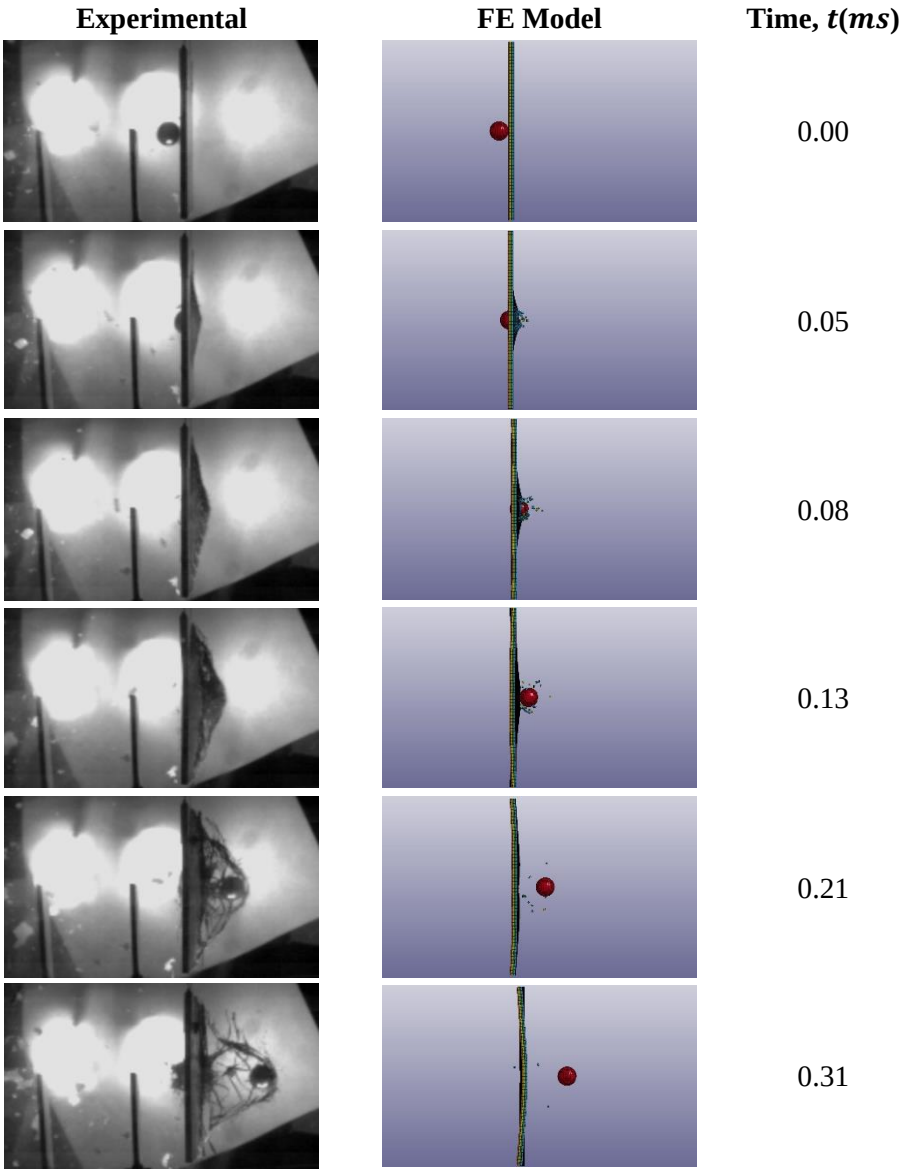

Figure 7. Timelapse of one of the HVI tests (experimental and numerical) where perforation was achieved, $V_i = 211.1 m/s$

The inconsistencies between the experimental and numerical results were contributed by a number of factors. First, the FE model which was developed using continuum shell elements, thus, the through-thickness properties of the impact plate were not fully accounted for. This results in the inferior performance of the FE model, especially at the lower impact velocities or nearer to the ballistic limit where damage is at its maximum. Furthermore, the delamination behaviour of the numerical model exhibited by Fig. 6 is also less pronounced when compared to the experimental gatherings. Once again, this is due to the inability of the continuum shells exhibiting the accurate delamination process (Fig. 10) of the specimen and fully capturing the energies released from matrix cracking.

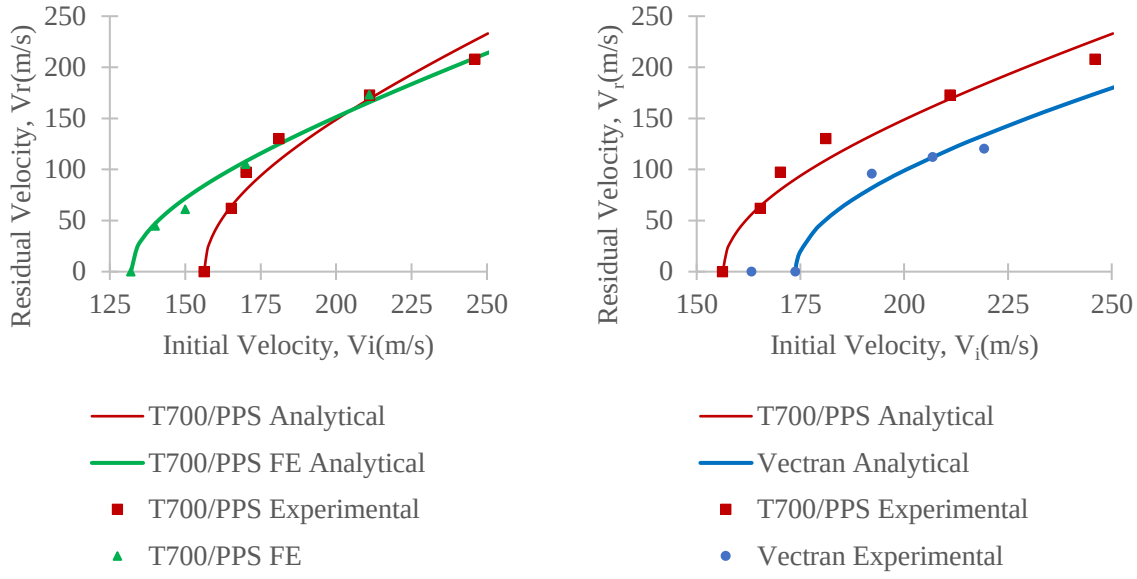

(a) (b)

Figure 8. (a) Ballistic curve of the T700/PPS composite system obtained from the experiments and FE simulations and (b) ballistic curve of the T700/PPS composite system and Vectran® [11] for comparison

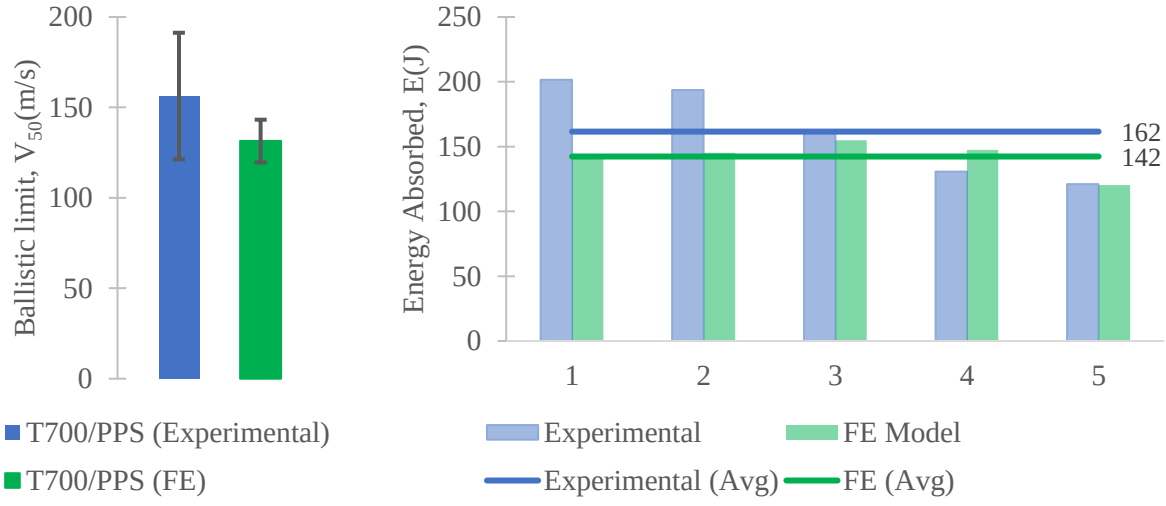

(a) (b)

Figure 9. (a) The ballistic limit, V_{50} obtained experimentally and numerically and (b) the energy absorbed by the panels following the HVI calculated from the experiments and FE simulations

Table 3. Coefficient of Variations (CV) of the Mechanical Properties of T700/PPS Composite

Mechanical Properties	Coefficient of Variation, CV (%)
Tensile	10.4
Compressive	5.5
In-plane Shear	4.2
Interlaminar Shear	11.4
Translaminar Shear	7.0

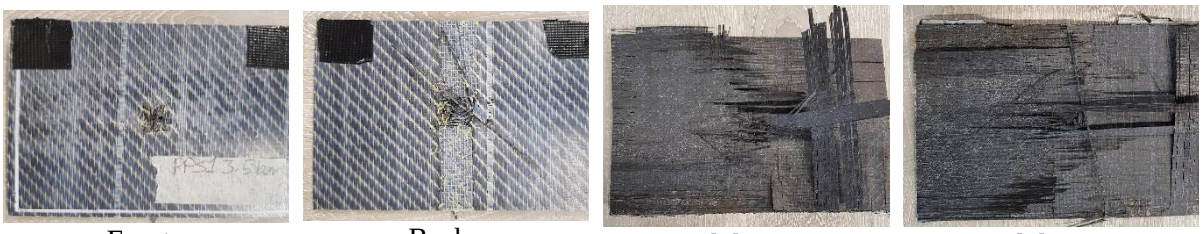

Front Back Midplane A Midplane B

Figure 10. The T700/PPS panel post impact

5. Conclusion

From the tests, the ballistic-limit velocity (V_{50}), which is an important parameter used to determine the penetration vulnerability, was determined (experimentally, $156.3m/s$ and numerically, $131.4m/s$). The predictions of the FE model are in good agreement with the experiments (approximately 12% with respect to the average impact energy absorbed). Furthermore, the ballistic performance of the T700/PPS is merely 10% lower of the superior Vectran® TS composite with similar fibre architecture [11]. Therefore, as CFRTP such as carbon/PPS is recycleable and more rapidly manufactured using out-of-autoclave (OOA) techniques than carbon fibre reinforced thermosetting (CFRTS). It can be concluded that the former offers a promising future and environmentally friendly composite material solutions for either automotive, aerospace or military applications.

References

[1] "UK-THERMOCOMP | CIC" [Online]. Available: http://the-cic.org.uk/uk-thermocomp.

[2] Steggall, P., 1999, "Developing Multiaxial Non-Crimp Reinforcements for the Cost Effective Solution," *Advanced Materials & Processes: Preparing for the New Millenium*, Society for the Advancement of Material and Process, pp. 341–354.

[3] Leong, K. H., Ramakrishna, S., Huang, Z. M., and Bibo, G. A., 2000, "Potential of Knitting for Engineering Composites - a Review," Compos. Part A Appl. Sci. Manuf., **31**(3), pp. 197–220.

[4] Mohsin, M. A. A., Iannucci, L., and Greenhalgh, E. S., 2018, "Testing, Modelling, Hybridisation and Fractography of Carbon Fibre Reinforced Thermoplastic Composites for the Automotive Industry," Imperial College London.

[5] Mohsin, M. A. A., Iannucci, L., and Greenhalgh, E. S., 2017, "Mode I Interlaminar Fracture Toughness Characterisation of Carbon Fibre Reinforced Thermoplastic Composites," *American Society for Composites (ASC) 32nd Annual Technical Conference*, American Society for Composites, West Lafayette, IN.

[6] Mohsin, M. A. A., Iannucci, L., and Greenhalgh, E. S., 2016, "Translaminar Fracture Toughness Characterisation of Carbon Reinforced Thermoplastic Composites," *ECCM17 - 17th European Conference on Composite Materials*, European Society for Composite Materials, Munich.

[7] Del Rosso, S., Iannucci, L., and Curtis, P. T., 2016, "On the Ballistic Impact Response of Microbraid Reinforced Polymer Composites," Compos. Struct., **137**, pp. 70–84.

[8] Ferriter, E. A., and Mcculloh, I. A., 2005, "Techniques Used to Estimate Limit Velocity in Ballistics Testing with Small Sample Size," *Proceedings of the 13th Annual U.S. Army Research Laboratory/United States Military Academy Technical Symposium, 72-95*.

[9] Lambert, J. P., and Jonas, G. H., 1976, *Towards Standardization in Terminal Ballistics Testing: Velocity Representation*.

[10] Recht, R. F., and Ipson, T. W., 1963, "Ballistic Perforation Dynamics," J. Appl. Mech., **30**(3), pp. 384–390.

[11] Syed Abdullah, S. I. B., 2018, "Operational Threats on Composites Aerostructures," Imperial College London.